Three-Dimensional Analysis of a MAGFET at 300 K and 77 K

Rodrigo Rodríguez-Torres, Robert Klima, and Siegfried Selberherr
Institute for Microelectronics, TU Wien
Gusshausstrasse 27-29, A-1040 Vienna, Austria
Rodrigo@iue.tuwien.ac.at

Edmundo A. Gutiérrez-D.
MCST, MOTOROLA-SPS
Puebla, MEXICO
Edmundo.Gutierrez@motorola.com

Abstract

Optimizing the electromagnetic performance of MOS-based magnetic sensors requires a deep knowledge of the electro-magnetic force interaction when the device is exposed to a magnetic field in a cryogenic ambient. Analytical approaches derived from numerical simulations are not appropriated under these conditions. Therefore, we use MINIMOS-NT to perform full 3D physics-based simulations of a two-drain MAGFET. The simulation results match very well to the available experimental data at 300 K and 77 K.

1. Introduction

A MAGFET is a MOSFET device with a split drain [1] designed in such a way that it is able to detect a magnetic field. When this magnetic field is applied perpendicular to the surface of the device, a current deflection appears as a result of the Lorentz force. If the MAGFET is a two-drain structure, then a differential current can be observed at those drains. This differential current is directly related to the sensitivity of the device, defined as

$$S = \frac{|I_{D1} - I_{D2}|}{(I_{D1} + I_{D2})|\overrightarrow{B}|} \tag{1}$$

where I_{D1} and I_{D2} are the currents at drain 1 and drain 2, and $\overrightarrow{B}$ the magnetic field strength.

To improve the magnetic sensitivity, two approaches are possible. The first one is to adapt the geometry, so the (W/L) and separation between the two drains gives a maximum sensitivity, and the second one is to cool the device down to 77 K, which increases the mobility upon which the carrier deflection ΔZ (See Fig. 1) depends on

$$\Delta Z = L\mu_n|\overrightarrow{B}| \tag{2}$$

2. Discretization Scheme

In a series of papers by Wachutka *et al.* [2, 3] the current equation comprising the magnetic field in the isothermal approximation for electrons reads

$$\overrightarrow{J_n} = -\sigma_n(\nabla\phi_n) - \sigma_n\frac{1}{1+(\mu_n^*\overrightarrow{B})^2}\{\mu_n^*\overrightarrow{B}\times\nabla\phi_n\} - \sigma_n\frac{\mu_n^*\overrightarrow{B}}{1+(\mu_n^*\overrightarrow{B})^2}\{\mu_n^*\overrightarrow{B}\times(\overrightarrow{B}\times\nabla\phi_n)\} \tag{3}$$

where σ_n is the electric conductivity of the electrons, $\nabla\phi_n$ the gradient of the electron quasi-Fermi potential, μ_n^* the hall mobility related to the normal mobility as $\mu_n^* = r_n\mu_n$ with r_n the Hall scattering factor, and $\overrightarrow{B}$ the magnetic field.

Along with the Poisson and continuity equations, a device under the presence of a magnetic field can be properly simulated under the driff- difussion approximation. The discretization of equation (3) was carried out following the general strategy depicted by Gajewski and Gärtner [4]. The vectorial product between the current density and the magnetic field is computed by considering a local coordinate system and the neighboring points. The discretization reads

$$J_B = \frac{s_k^T(I + N^T(\beta\beta^T + \beta_\times)N^{-T})J_0}{1+\beta^2} \tag{4}$$

where J_B are the projection currents along the meshing lines in the local coordinate system with the magnetic field, J_0 are the projection currents along the meshing lines in the local coordinate system without magnetic field, s_k the distance ratios, I the unitary matrix, β the dimensionless product between magnetic field and hall mobility, $\beta_\times$ is a linear operator that combined with the $\beta\beta^T$ gives the matrix representation of a vectorial product, and N the matrix composed with the unitary vectors of the local coordinate system. This discretization scheme was sucessfully implemented in MINIMOS-NT.

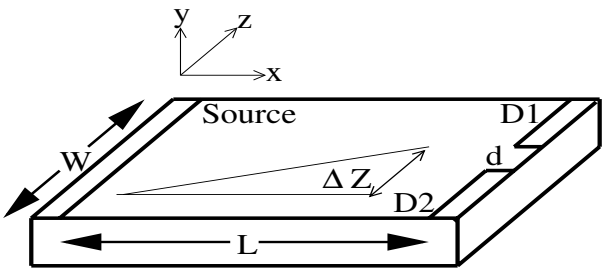

Figure 1. A view of the simulated MAGFET.

3. Simulated Structure

Fig. 1 depicts the actual simulated structure. It is an N-channel MAGFET with a substrate doping of 1×10^{15} cm^{-3}, an oxide thickness of 60 nm. The device width is 100 μm and the length is 125 μm. The separation between the drains is 10 μm. Fig. 2 shows the electrical behavior of the device with and without a magnetic field (50 mT), and a simulation at the same operating conditions (0.5 V drain to source voltage). The simulation results fit very well the experimental data. At 4.96 V, the magnetic field is turned off and because of the hysteresis present in the magnetic field generator, the simulation does not reproduce this part of the measurements. The Hall scattering factor used for electrons was set to 1.15 [5].

The Lorentz force acts on the moving charges. So it is expected that the current distribution inside the MAGFET device changes when a magnetic field is applied.

$$\Delta I_D = |I_{D1} - I_{D2}| = \frac{I_{D1} + I_{D2}}{L} \Delta Z = (I_{D1} + I_{D2}) \mu |\vec{B}| \quad (5)$$

In order to *see* such a change, the MAGFET is simulated with a gate to source voltage of 4.95 V and a drain to source voltage of 1 V. The Hall scattering factor used for electrons was set to 1.15 [5]. Fig. 5, 6, and 7 show the current density in cuts at 30 μm, 60 μm, and 90 μm from the source without magnetic field. It is clear from these figures that the current is equally distributed in both drains when no magnetic field is present.

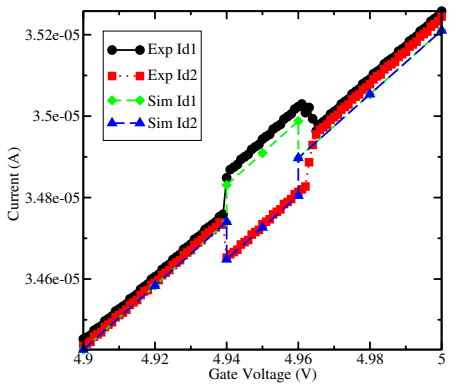

Figure 2. Drain Currents for different gate voltages with and without magnetic field.

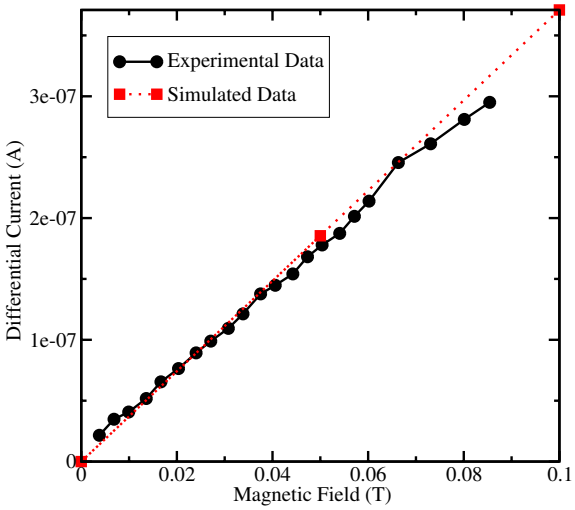

Figure 3. Differential Current at 300 K.

A magnetic field of 40 mT normal to the surface and perpendicular to the channel current, flowing from the substrate up to the gate, is used in the simulations. At x=30 μm and 60 μm a current deflection is not easily visualized (Figs. 8 and 9). However, at 90 μm (Fig. 10) the charge deflection is easily observed. These results confirms that, with a same device width, carrier deflection is more pronounced in larger devices. If the magnetic field direction is reversed, the electrons will pile up at the other drain side.

At 77 K the current density increases by a factor of 4 due to the increase of carrier mobility. This makes more difficult to visualize the carrier deflection (Figs. 11, 12, and 13). However, the simulated differential current at the contacts show an increase in the absolute value as seen from Figure 4. The carrier deflection ΔZ is directly dependent upon the carrier mobility. Therefore, the differential current increases at lower temperatures. The used Hall scattering factor was set to 2 [6].

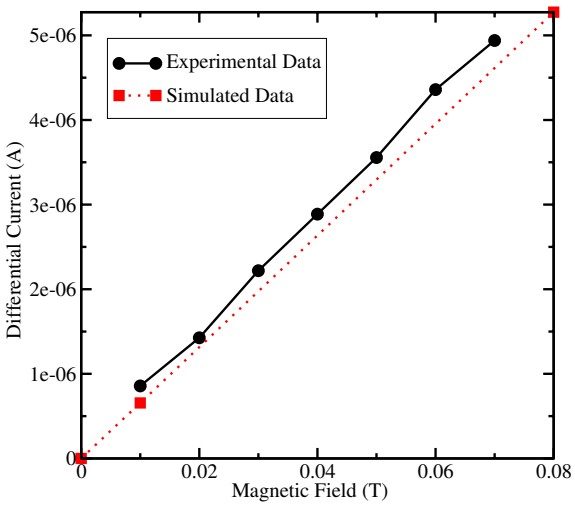

Figure 4. Differential Current at 77 K.

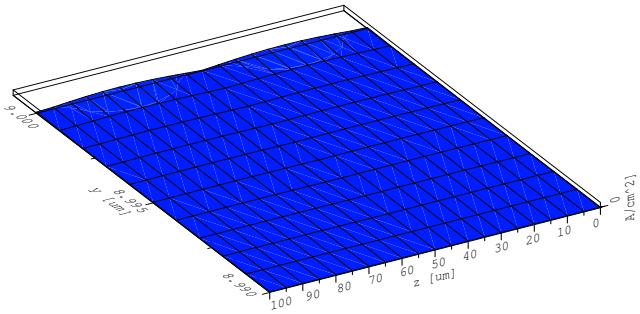

Figure 5. Current Density (300 K, 0 mT) at x=30 μm.

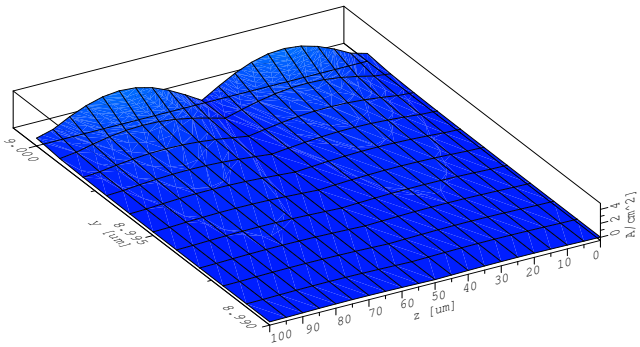

Figure 6. Current Density (300 K, 0 mT) at x=60 μm.

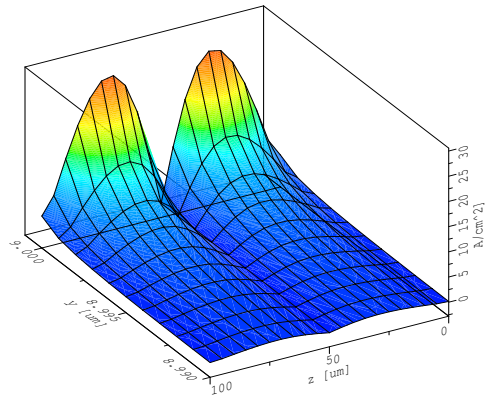

Figure 7. Current Density (300 K, 0 mT) at x=90 μm.

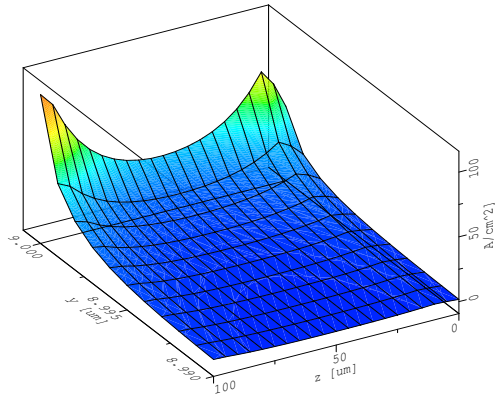

Figure 8. Current Density (300 K, 40 mT) at x=30 μm.

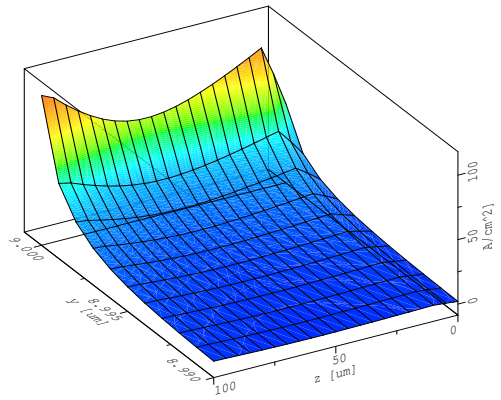

Figure 9. Current Density (300 K, 40 mT) at x=60 μm.

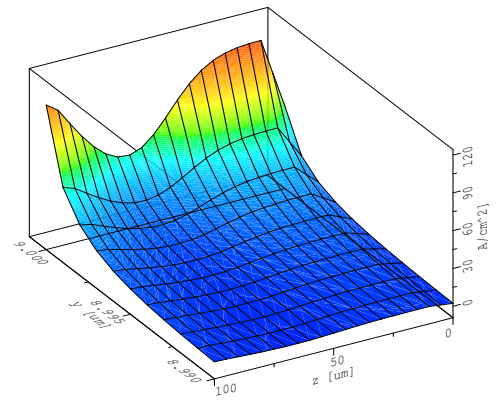

Figure 10. Current Density (300 K, 40 mT) at x=90 μm.

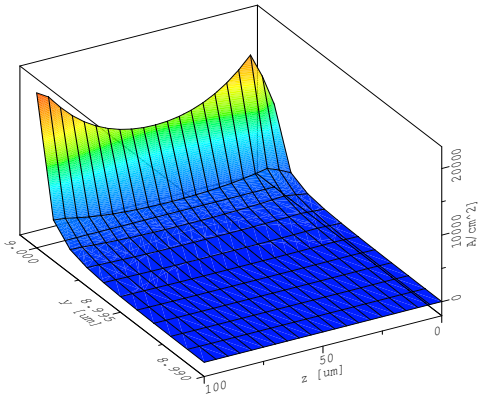

Figure 11. Current Density (77 K, 40 mT) at x=30 μm.

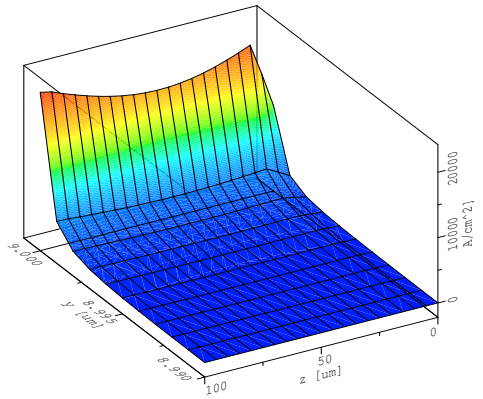

Figure 12. Current Density (77 K, 40 mT) at x=60 μm.

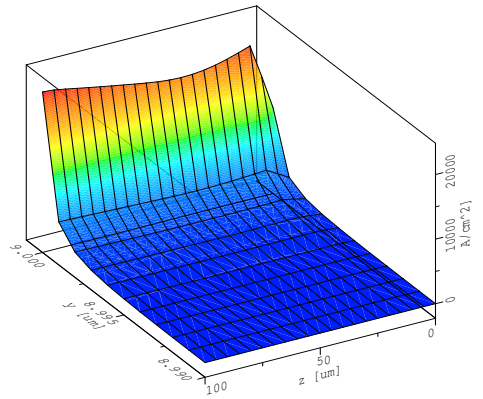

Figure 13. Current Density (77 K, 40 mT) at x=90 μm.

4. Measurements

The detection of a magnetic field via a MAGFET is carried out, in the case of a two-drain structure, by means of measuring the diferential current between both drains. Fig. 3 shows a comparison between the simulation results and the experimental data for room temperature. Fig. 4 shows the same diferential current at 77 K.

At room temperature the simulation matchs perfectly the experimental data. At 77 K the simulation results are close to the measurements. This differential current is a function of the current magnitude, directly related to the carrier mobility, and the Hall scattering factor. Because the electrical characteristics of the MAGFET were matched before carrying out the simulation with magnetic field, it is clear that the Hall scattering factor has a great impact in the simulation.

5. Conclusions

The analysis and simulation of a two-drain MAGFET have been successfully carried out with MINIMOS-NT in three dimensions. The involved vector product between the current density and the magnetic field has been computed by means of a linear combination of the different current projections along the meshing lines of the simulation grid. Using this discretization, a two-drain MAGFET structure has been simulated and the simulation results show a good agreement with the experimental data for two different temperatures.

6. Acknowledgements

We are in debt to the Electronics Department of the National Institute for Astrophysics, Optics, and Electronics (INAOE), Tonantzintla, Puebla, Mexico for the device fabrication and measurement facilities.

[1] H. P. Baltes and R. S. Popović, "Integrated semiconductor magnetic field sensors," *Proceedings of the IEEE*, vol. 74, August 1986, pp. 1107–1132.

[2] S. Rudin, G. Wachutka, and H. Baltes, "Thermal effects in magnetic microsensors modeling," *Sensors and Actuators A*, vol. 27, 1991, pp. 731–735.

[3] G. Wachutka, "Unified framework for thermal electrical, magnetic, and optical semiconductor device modeling," *COMPEL*, vol. 10, no. 4, 1991, pp. 311–321.

[4] H. Gajewski and K. Gärtner, "On the discretization of van roosbroeck's equations with magnetic field," *ZAMM*, vol. 76, no. 5, 1996, pp. 247–264.

[5] C. Riccobene, *Multidimensional Analysis of Galvanomagnetic Effects in Magnetotransistors*. PhD thesis, Eidgenössiche Technische Hochschule Zürich, 1995.

[6] C. Jungemann, D. Dudenbostel, and B. Meinerzhagen, "Hall factors of SI NMOS inversion layers for MAGFET modeling," *IEEE Transactions on Electron Devices*, vol. 46, August 1999, pp. 1803–1804.